# Temperature dependent luminescence characteristics of $KBe_2BO_3F_2$ and $RbBe_2BO_3F_2$



2015 IOP Conf. Ser.: Mater. Sci. Eng. 80 012015

(http://iopscience.iop.org/1757-899X/80/1/012015)

IOP Conf. Series: Materials Science and Engineering **80** (2015) 012015 doi:10.1088/1757-899X/80/1/012015

# Temperature dependent luminescence characteristics of $KBe_2BO_3F_2$ and $RbBe_2BO_3F_2$

**J Martincik[1,2], V Babin[1], L Liu[3], X Wang[3], C T Chen[3], A Beitlerova[1], E Mihokova[1], and M Nikl[1]**

[1] Institute of Physics AS CR, Cukrovarnicka 10, Prague, Czech Republic
[2] FNSPE, Czech Technical University, Prague, Czech Republic
[3] Beijing center for crystal research and development, Technical Institute of Physics and Chemistry, Chinese Academy of Sciences, P.O. Box 2711, Beijing, China

E-mail: jiri.martincik@fjfi.cvut.cz

**Abstract.** This paper reports on a study of the luminescence characteristics of $KBe_2BO_3F_2$ (KBBF) and $RbBe_2BO_3F_2$(RBBF) crystals in UV/visible spectral range. The KBBF crystals are very popular for their nonlinear optical properties, however they have a potential to be used as scintillators for neutron detection. To determine the effectiveness of KBBF scintillation we combine the results from measurements of optical absorption; radioluminescence; light yield; photoluminescence and decay kinetics in the temperature range 8-330 K. Temperature dependence of luminescence in KBBF crystals is discussed.

## 1. Introduction

The $KBe_2BO_3F_2$ (KBBF) crystals have been known since 1968 and today they are very popular for their nonlinear optical properties and large band gap enabling their application for frequency multiplication down to VUV spectral region, see e.g. [1, 2]. The large band gap of the host KBBF can incorporate many rare earth ions to alter its luminescence properties for applications such as lasers or scintillators [3]. Research of borate compound system is very intensive and many new structure types with rare earth elements were discovered [4].

The investigation of various borate crystals [5, 6, 7] shows that these materials are suitable for neutron detection with efficiency comparable with other systems used for neutron detection [8].

Our research is focused on examining the effectiveness of scintillation of KBBF crystals in order to find a suitable candidate for scintillator for neutron detection. Our interest is the luminescence of defects and its temperature dependence in the UV/visible part of spectra. Only few papers dealing with investigation of the luminescence characteristics of KBBF are published [9].

## 2. Experimental details

KBBF and $RbBe_2BO_3F_2$ (RBBF) crystals were grown by a localized spontaneous nucleation technique without seeding by the flux method [10]. Polycrystalline KBBF powders were mixed with KF and $B_2O_3$ in a proper ratio and melted at around 750 °C. The crystals were grown at a cooling rate of 1.0-3.0 °C/d. The cooling range was more than 60 °C and the growth period was about two months. The growth procedure was similar for RBBF crystal growth by using

a NaF-$B_2O_3$ flux system. These crystals could also be grown by the hydrothermal method. The growth details can be found in [11, 12]. After the growth had been finished, the crystals were cut into small pieces and optically polished for luminescence measurements. Samples are cut into sizes of about 5×5 $mm^2$ with thicknesses varied from 0.2 mm to 1.5 mm. At room temperature, the KBBF crystals are chemically stable and nonhygroscopic with the density of about 2.4 $g{\cdot}cm^{-3}$. Eleven samples grown by different methods are prepared and optically polished as listed in table 1.

**Table 1.** Composition of KBBF and RBBF crystals; h-means hydrothermal-grown; f-means flux-grown.

| Number | 1 | 2 | 3 | 4 | 5 | 6 | 7-11 |
|---|---|---|---|---|---|---|---|
| Composition | h-RBBF | h-RBBF | h-KBBF | f-KBBF | f-KBBF | f-RBBF | f-KBBF |
| Growth temp. (°C) | 430 | 430 | 450 | 720 | 720 | 740 | 700 |
| Flux system | $Rb_2CO_3$ | $Rb_2CO_3$ | KOH | KF-$B_2O_3$ | KF-$B_2O_3$ | NaF-$B_2O_3$ | KF-$K_2O$-$B_2O_3$ |

Optical absorption spectra of all samples were measured at spectrometer Shimadzu 3101PC. Radioluminescence, photoluminescence and decay kinetics were measured by the custom made spectrofluorometer Horiba Jobin Yvon 5000M with a photon counting detector TBX-04 (IBH Scotland). The steady-state emission and excitation spectra of the KBBF were measured at the same conditions in the temperature range 8-330 K. The measurements were performed in a closed cycle cryostat (Janis). All spectra were corrected for instrumental distortions.

Luminescence decay kinetics in the microsecond time range was measured at 8-330 K by the same set-up under excitation by a xenon flash lamp FX-1152 (EG&G) and using the multichannel scaling method. A deconvolution procedure was used to extract the true decay time data using the SpectraSolve software package (Ames Photonics).

Light yield under an alpha particle excitation from $^{241}Am$ radioisotope was measured by the method of pulse-height spectra. Using a silicon grease, the sample is optically coupled to a hybrid photomultiplier (HPMT) [13] model DEP PPO 475B. Signal from HPMT is processed by spectroscopy amplifier ORTEC 672 and multichannel buffer ORTEC 927TM. Pulse-height spectrum is displayed on PC. All measurements were performed at room temperature.

## 3. Results and discussion

Our results combine the measurements of absorption, radioluminescence and photoluminescence emission and excitation spectra. We mainly focus on the luminescence band around 350 nm and its temperature dependence within 8-330 K. Furthermore, the decay kinetics of emission transitions in visible range in KBBF crystals was also studied.

Radioluminescence spectra in figure 1 are very similar to those of photoluminescence presented in [9], peaking at about 310-320 nm (4 eV). In some samples (RBBF-1, RBBF-6) their integral efficiency is quite high, about 300-400 % of that of $BiGe_3O_{12}$ (BGO) standard scintillator sample. However, light yield measurements of two most intensely emitting samples, no. 1 and 6 provided the values which are approximately an order of magnitude lower than those of the BGO standard scintillator. This result points to intense slow decay components in the KBBF scintillation response. This assessment is supported by strongly increasing LY value with increasing shaping time and by the presence of slow decay components in photoluminescence decays down to tens of microseconds. The results are reported in table 2.

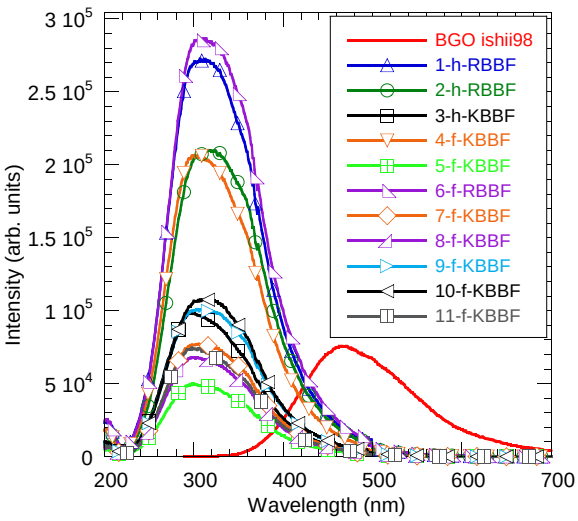


**Figure 1.** Radioluminescence spectra (excited by X-ray source, 40 kv, 15 mA).

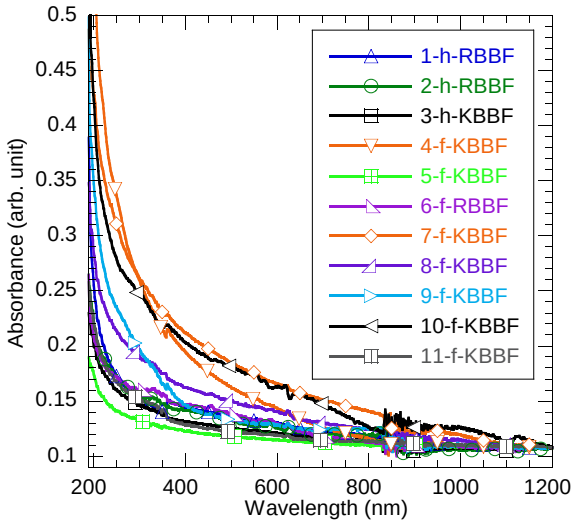


**Figure 2.** Optical absorption spectra of the sample set.

Slowly increasing absorbance in figure 2 towards shorter wavelengths can be due to scattering surface or any scattering inclusions in the samples without any apparent absorption bands. From the point of view of light scattering KBBF no. 5 is the best (least scattering).

**Table 2.** Scintillation properties of h-RBBF-1 and f-RBBF-6 crystals. Pulse height spectra were excited by $\alpha$-particles from $^{241}$Am source with thin Palladium layer at various shaping time from 0.5 to 10 $\mu$s. Number of photoelectrons ($N_{phels}$/MeV) was calculated from used energy of $^{241}$Am with layer 4.8 MeV)

| | h-RBBF-1 | | | | | f-RBBF-6 | | | | |
|---|---|---|---|---|---|---|---|---|---|---|
| Shaping time ($\mu$s) | 0.5 | 1 | 2 | 3 | 6 | 0.5 | 1 | 2 | 3 | 6 |
| $N_{phels}$ | 30 | 28.6 | 34.5 | 39.3 | 56 | 32.3 | 42.3 | 51.6 | 51 | 90.5 |
| FWHM (%) | 34.3 | 43.7 | ≈30 | 45.9 | 39.8 | 36.8 | ≈40 | ≈30 | ≈30 | ≈30 |
| LY per MeV ($N_{phels}$/1MeV) | 6.25 | 5.96 | 7.19 | 8.19 | 11.67 | 6.73 | 8.82 | 10.75 | 10.63 | 18.85 |

To deeper investigate the luminescence of defects we measured the decay kinetics and temperature dependence of the luminescence band peaking at about 350 nm.

The main interest was focused on both the changes of emission intensity and shortening of decay components with increasing temperature. Temperature dependence of emission characteristics was measured in the range 8-330 K.

Temperature dependence of photoluminescence spectra is shown in figure 3. There seem to be a slight shift of the position of the emission maximum between the low and intermediate temperatures pointing to the composed character of the PL spectrum. This observation was further pursued by measurement of PL decays.

Photoluminescence decays were not single exponential and could only be fit by the sum of several exponentials. Figure 4 presents an example of the photoluminescence decay fit by three exponential function. The slowest component is very weak, therefore two exponential functions were considered for the fits of temperature dependence of PL decays.

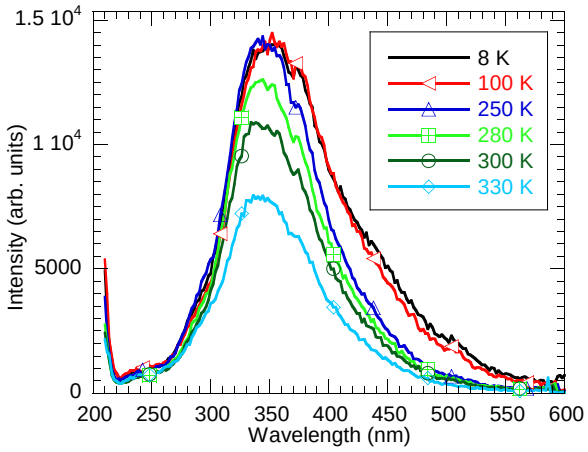


**Figure 3.** Photoluminescence spectra for exc=195 nm of sample no. 2.

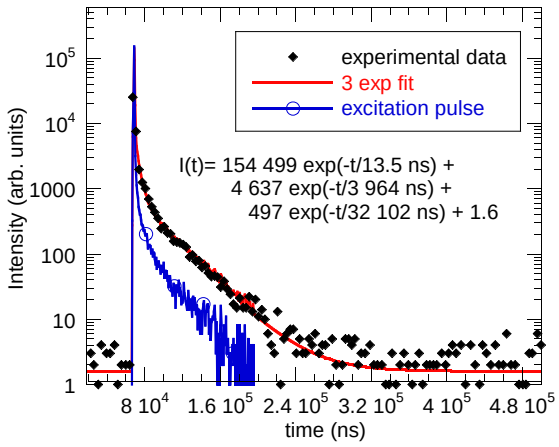


**Figure 4.** Photoluminescence decay under exc=195 nm and em=237 nm of sample no. 2. Solid line is the approximation made by convolution of instrumental response to excitation pulse and function I(t).

The decay times obtained from two-exponential approximation of PL decays as a function of temperature are shown in figure 5.

The two components of the decay indeed do not seem to be associated with the same luminescence center. This feature confirms a composed character of the PL spectrum. The behavior of fast decay can be satisfactorily described by a phenomenological model of the luminescence center consisted of three excited state levels (see the scheme in figure 6a). Observed decay corresponds to the slowest decay component of the luminescence center. Similar model was used in [14].

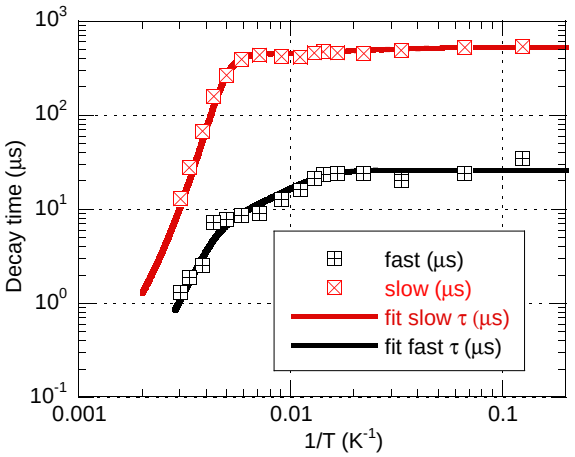


**Figure 5.** Temperature dependence of decay times of sample no. 2, exc=195 nm, em=350 nm; temperature range 3-330 K. Squares are experimental data, solid lines are the fits using models desribed in the text.

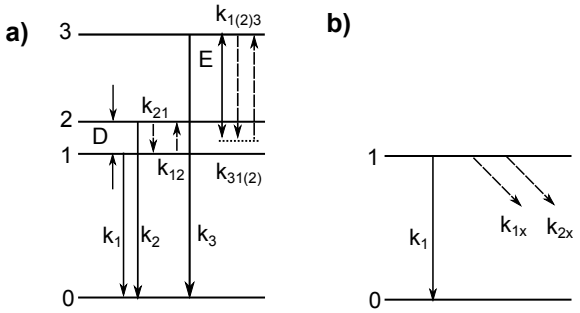


**Figure 6.** Energy level diagrams used for the description of decay kinetics. a) fast decay component model; b) slow decay component model

According to such model the shortening of the decay time with increasing temperature is caused by thermally stimulated non-radiative transitions between the excited state levels as depicted in the scheme in figure 6a. The time evolution of the populations $N_1$, $N_2$ and $N_3$ of the excited levels 1, 2 and 3, respectively, can be described by the following rate equations:

$$\begin{aligned}\frac{dN_1}{dt} &= -k_1N_1 - k_{12}N_1 - k_{13}N_1 + k_{21}N_2 + k_{31}N_3\\ \frac{dN_2}{dt} &= -k_2N_2 - k_{21}N_2 - k_{23}N_2 + k_{12}N_1 + k_{32}N_3\\ \frac{dN_3}{dt} &= -k_3N_3 - k_{31}N_3 - k_{32}N_3 + k_{13}N_1 + k_{23}N_2\end{aligned} \tag{1}$$

$$k_{21} = K\left(n+1\right),\ k_{12} = Kn,\ n = \frac{1}{exp(\frac{D}{k_bT}) - 1} \tag{2}$$

$$k_{31} = K^{'}\left(n^{'}+1\right),\ k_{31} = K^{'}n^{'},\ n^{'} = \frac{1}{exp\left(\frac{E}{k_bT}\right) - 1} \tag{3}$$

Here $K$, $n$ and $D$ are the zero-temperature transition rate between the levels 1 and 2, the Bose-Einstein factor and energy spacing between the levels, respectively.

The parameters of the fit shown as a black solid line in figure 5 are presented in table 3.

**Table 3.** Parameters of the fast decay (value a) and slow decay (value b) component fit.

| Parameter | $\mathbf{k_1}$ | $\mathbf{k_2}$ | $\mathbf{k_3}$ | **K** | **K'** | **E** | **D** |
|---|---|---|---|---|---|---|---|
| value (a) | 3.8e4 $s^{-1}$ | 5e5 $s^{-1}$ | 1e9 $s^{-1}$ | 5e6 $s^{-1}$ | 2e8 $s^{-1}$ | 150 meV | 25 meV |
| Parameter | $\mathbf{k_1}$ | **K** | $\mathbf{K_{1x}}$ | $\mathbf{K_{2x}}$ | $\mathbf{E_{1x}}$ | $\mathbf{E_{2x}}$ | |
| value (b) | 1.9e3 $s^{-1}$ | 5e2 $s^{-1}$ | 5e8 $s^{-1}$ | 5e7 $s^{-1}$ | 5 meV | 180 meV | |

Slow decay points to deexcitation of one level with two quenching channels (see figure 6b). The nonradiative decay rate can be described by a simple barrier transition model:

$$k_{ix} = K_{ix}exp\left(-\frac{E_{ix}}{k_bT}\right),\ i = 1, 2 \tag{4}$$

with $K_{ix}$ being a frequency factor and $E_{ix}$ is the height of the barrier. Parameters of the fit of the slow PL decay from figure 6b are presented in table 3.

Though the exact nature of the emission centres responsible for luminescence characteristics is not entirely clear, due to the excitation well below the band gap the luminescence process must be related to a defect and/or deeply trapped exciton. One may even consider that both emissions, i.e. that of the defect energy levels and that of the exciton contribute to the observed complex luminescence bands. Similarity of the radioluminescence band shape in all the samples suggest that the luminescence centres are independent on the chemical composition and doping of the samples, i.e. related to defects which are possibly specific for the growth technology used.

## 4. Conclusions

All the studied samples of single crystal borates show an emission band in UV region peaking around 310-320 nm under X-ray excitation, consistent with [3]. The intensity of samples 1, 2, 4 and 6 exceeds that of BGO standard scintillator. However, light yield measurements under alpha particle excitation of two most intensely emitting samples no. 1 and 6 provide the values which are approximately an order of magnitude lower compared to that of BGO measured in the same conditions. It points to intense slow decay components in the scintillation response. This is supported by strongly increasing LY values with increasing shaping time and by the presence of slow decay components in photoluminescence decays down to tens of microseconds.

The study of temperature dependence of the PL spectra and decays of KBBF sample no. 2 suggests that the emission band peaking at about 350 nm is composed of at least two subbands. Given the subband excitation the defect and/or deeply trapped exciton are proposed as its origin, but further study is necessary.

## Acknowledgments

Financial support of Czech TACR TA01011017 project and the National Natural Science Foundation of China (Grant No. 6113800451402316) is gratefully acknowledged.

## References

[1] Lin Z, Wang Z, Chen C T, Chen S K and Lee M H 2003 Mechanism for linear and nonlinear optical effects in $KBe_2BO_3F_2$ (KBBF) crystal *Chem. Phys. Lett.* **367** 523
[2] Chen C T, Wang G L, Wang X Y, Xu Z Y 2009 *Appl. Phys. B* **97** 9-25
[3] Ogorodnikov I N, Poryvay N E, Sedunova I N, Tomachev A V, Yavetskiy R P 2011 Thermally stimulated recombination processes and luminescence in $Li_6(Y,Gd,Eu)(BO_3)_3$ crystals *Physics of the Solid State* **53** 263-270
[4] Gao J H, Li R K, 2008 Potassium rich rare earth (RE) borates $K_3RE(BO_3)_2$ *Sol. St. Sci.* **10** 26-30
[5] Engels R, Reinartz R, Schelten J Czirr B 2000 Thermal neutron netection with the lithium borate scintillator *Nucl. Sci. IEEE Transac.* **47** 948-951
[6] van Eijk C.W.E 2004 Inorganic scintillators for thermal neutron detection *Rad. Meas.* **38** 337-342
[7] Singh A K, Tyagi M, Singh S G, Desai D G, Sen S, Nayak B K, Urffer M, Melcher C L, Gadkari C S 2013 Cerium doped Lithium Gadolinium Borate: A neutron Scintillator *Proceedings of the DAE Symp. on Nucl. Phys.* **58** 960
[8] Engels R, Kemmerling G, Rongen H, Schelten J, Cooper R 2002 Comparison of neutron scintillation detectors with a $^3$He proportional counter for the spallation neutron source (SNS) *IEEE Trans. on Nucl. Sci.* **49** 923-925
[9] Ogorodnikov I N, Pustovarov V A, Yakovlev S A, Isaenko L I and Zhurkov S A 2012 Luminescence and electronic excitations in $KBe_2BO_3F_2$ crystals *ISSN 1063-7834 Phys. of the Solid State* **54**4 735–740
[10] Wang X, Yan X, Luo S and Chen Ch 2011 Flux growth of large KBBF crystals by localized spontaneous nucleation *J. of Cryst. Growth* **318** 610-612
[11] Zhou H, He X, Zhou W, Hu Z 2011 Hydrothermal growth of KBBF crystals from KOH solution *Journal of Crystal Growth* **318** 613-617
[12] Liu L, Zhou H, He X, Zhang X 2012 Hydrothermal growth and optical properties of RbBe2BO3F2 crystals *Journal of Crystal Growth* **348** 60-64
[13] D'Ambrosio C, Leutz H 2003 *Nucl. Inst. Meth. A* **501** 463-498
[14] Babin V, Gorbenko V, Krasnikov A, Makhov A, Mihokova E, Nikl M, Zazubovich S, Zorenko Y 2012 *Phys. Status Solidi* B **249** 5 1039–1045